

# Aberrant CpG Islands' Hypermethylation of ABCB1 in Mesenchymal Stem Cells of Patients with Steroid-associated Osteonecrosis

Zhibo Sun, Shuhua Yang, Shunan Ye, Yukun Zhang, Weihua Xu, Bo Zhang, Xianzhe Liu, Fengbo Mo, and Wenbin Hua

**ABSTRACT.** *Objective.* Patients carrying an ABCB1 polymorphism have a higher risk of developing osteonecrosis of the femoral head (ONFH). We investigated whether aberrant dinucleotide CpG islands' hypermethylation of ABCB1 gene existed in mesenchymal stem cells (MSC) of patients with ONFH, which results in cell dysfunction.

*Methods.* Bone marrow was collected from the proximal femur of patients with glucocorticoid (GC)-associated ONFH (n = 22) and patients with new femoral neck fractures (n = 25). MSC were isolated by density gradient centrifugation. We investigated cell viability, intracellular reactive oxygen species (ROS) level, mitochondrial membrane potential (MMP), the amount of P-glycoprotein (P-gp) and ABCB1 transcripts, and methylation at CpG islands of ABCB1 promoter from both the femoral neck fractures group and the GC-associated ONFH group treated with or without the DNA methyltransferase inhibitor, 5'-Aza-2-deoxycytidine (5'-Aza-dC).

*Results.* We observed that MSC from GC-associated ONFH groups showed reduced proliferation ability, elevated ROS levels, and depressed MMP when compared with the other 2 groups. Low levels of P-gp and ABCB1 transcript, as well as ABCB1 gene hypermethylation, in patients with GC-associated ONFH were also noted. Treatment with 5'-Aza-dC rapidly restored ABCB1 expression. Analysis of general expression revealed that aberrant CpG islands' hypermethylation of ABCB1 caused sensitivity to GC and induced changes in the proliferation and oxidative stress of MSC under GC administration.

*Conclusion.* These data suggest that aberrant CpG islands' hypermethylation of ABCB1 gene may be responsible for individual differences in the development of GC-associated ONFH. (First Release Sept 15 2013; J Rheumatol 2013;40:1913–20; doi:10.3899/jrheum.130191)

## Key Indexing Terms:

HYPERMETHYLATION

ABCB1

MESENCHYMAL STEM CELLS

STEROID-ASSOCIATED OSTEONECROSIS

Nontraumatic osteonecrosis of the femoral head (ONFH) is considered to be part of a multifactorial, heterogeneous group of disorders that lead to a common pathway and mechanical failure of the femoral head during later stages<sup>1,2,3</sup>. In China, glucocorticoid (GC)-induced ONFH ranks first among the known risk factors for nontraumatic ONFH, because GC is widely used in daily clinical practice. Steroids are administered in large doses or on a long-term basis to patients with collagen diseases such as systemic

lupus erythematosus (SLE), rheumatoid arthritis (RA), asthma, and after organ transplants. Opportunities to treat these diseases are increasing; accordingly, it is predicted that the incidence of GC-induced ONFH will also increase. In spite of many studies since this condition was first described by Pietrogrande and Mastomaro<sup>4</sup>, the exact pathogenesis of femoral head osteonecrosis related to GC remains uncertain.

There are several alternative mechanisms responsible for GC-induced ONFH, such as fat embolisation<sup>5</sup>, intra-medullary pressure changes<sup>6</sup>, modified artery constriction<sup>7,8</sup>, circulatory impairment<sup>9</sup>, coagulation disorders<sup>10</sup>, and cell dysfunction<sup>11,12,13</sup>. However, none can explain the underlying mechanism alone. Because the same protocol for steroid administration induces ONFH in some patients, individual differences in steroid sensitivity may exist.

Epigenetics, as an effective method to study the interplay between environmental signals and the genome, have received a great deal of attention recently. Epigenetic mechanisms play crucial roles in the control of gene activity and nuclear architecture<sup>14</sup>. The most widely studied

From the Department of Orthopedics, Union Hospital, Tongji Medical College, Huazhong University of Science and Technology, Wuhan, Hubei, China.

Supported by a grant from the National Natural Science Foundation of China (No. 81171750).

Z. Sun, PhD; S. Yang, MD, Professor; S. Ye, MD, Professor; Y. Zhang, PhD, Professor; W. Xu, MD, Professor; B. Zhang, PhD; X. Liu, MD; F. Mo, MD; W. Hua, MD, Department of Orthopedics, Union Hospital, Tongji Medical College, Huazhong University of Science and Technology.

Address correspondence to Dr. S. Ye, Wuhan Union Hospital, Jiefang Avenue 1277, Jiangnan District, Wuhan, 430022, China.

E-mail: shunanye@126.com or Dr. S. Yang, shuhuayang196@126.com

Accepted for publication July 15, 2013.

epigenetic modification in humans is the cytosine methylation of DNA within the dinucleotide CpG. Emerging evidence shows that epigenetics may be a candidate mechanism for individual differences<sup>15</sup>.

P-glycoprotein (P-gp), encoded by ABCB1, plays an important role in absorption and distribution of drugs and can protect normal cells or tissues from hazards. As a member of the adenosine triphosphate-binding cassette transporter super-family, P-gp can transport substrates from the inside to the outside of cells using adenosine triphosphate as an energy source. Glucocorticoid, orally administered to patients, was shown to be a substrate for P-gp<sup>16</sup>. Studies have found that P-gp is closely related to the development of steroid-induced ONFH<sup>17</sup>. In particular, increased P-gp activity was found to be a statistically relevant marker for low risk of developing steroid-induced ONFH<sup>18</sup>.

Mesenchymal stem cells (MSC), one of the multipotent stem cells, were originally identified in adult bone marrow<sup>19</sup>. They can proliferate and differentiate into multiple mesodermal lineages such as osteoblasts<sup>20</sup>, cardiocytes<sup>21</sup>, chondrocytes<sup>22,23</sup>, and adipocytes<sup>24</sup>. In the GC-induced ONFH, the decreased number and hypoproliferative activity of MSC of the femoral head, neck, and metaphysis is responsible for the poor self-repair and bad prognosis. MSC dysfunction is considered a principal mechanism in the development of ONFH.

In our study, we focused on the transport protein P-gp in MSC and investigated whether aberrant CpG islands' hypermethylation of ABCB1 was involved in the development of GC-induced ONFH. Further, we examined methylation at CpG islands of ABCB1 using bisulfite sequencing and investigated whether demethylation of ABCB1 would improve cell viability and oxidative stress status. We attempted to confirm that aberrant hypermethylation of ABCB1 is related to the development of GC-induced ONFH.

## MATERIALS AND METHODS

**Patients.** Our study was approved by the Ethics Committee of Wuhan Union Hospital, Wuhan, China. Between July 2011 and September 2012, 22 patients (10 men, 12 women; mean age 49.3, range 39-65 yrs) with GC-induced ONFH were selected at the hospital, and 25 subjects with femoral neck fractures (15 men and 10 women; mean age 52.3, range 36-68 yrs) were enrolled as controls. Clinical characteristics for all participants are summarized in Table 1. For GC-induced ONFH, the steroid exposure threshold is 1800 mg GC or its equivalent over 4 weeks<sup>25</sup>. After written informed consent was obtained from patients, bone marrow aspirates (5 ml) were procured from the proximal end of femur while inserting the tapered awl into the femoral canal during hip replacement surgery.

**Cell culture.** Human MSC (hMSC) were isolated from bone marrow aspirates and cultured, as previously described<sup>26</sup>. Adherent cells were cultured for 12 to 14 days until they attained a confluence > 80%. The cells were then digested using a solution of 0.25% trypsin and 0.02% EDTA (Invitrogen), and replated at a 1:2 dilution for the initial subculture. The hMSC underwent this treatment 3 times before they were collected for further use. The hMSC used for each experiment were from the bone marrow aspirates of all patients.

**Cell viability measurement.** The hMSC were plated in the 96-well plate at

Table 1. Clinical characteristics of the subjects.

Characteristics	ONFH, n = 22	Controls, n = 25	p
Age, yrs	49.3 ± 8.6	52.3 ± 8.7	0.243
Sex, male/female	10/12	15/10	0.319
Body mass index, kg/m <sup>2</sup>	25.4 ± 2.7	24.3 ± 2.9	0.180
Hypertension	4 (18.5%)	4 (16.0%)	0.843
Smoker	8 (36.4%)	9 (36.0%)	0.979
Alcoholism	3 (13.6%)	4 (16%)	0.820
GC medication	22 (100%)	2 (8%)	
Total cholesterol, mmol/l	5.47 ± 0.59	4.86 ± 0.83	0.006
LDL cholesterol, mmol/l	3.30 ± 0.37	3.12 ± 0.35	0.120
HDL cholesterol, mmol/l	1.17 ± 0.35	1.26 ± 0.40	0.394
Triglycerides, mmol/l	1.75 ± 0.38	1.60 ± 0.32	0.178

Data are mean ± SD. Statistical significances of differences (p) between groups were determined by paired Student's t test (continuous values) and chi-square test (categorical values). ONFH: osteonecrosis of the femoral head; GC: glucocorticoid; LDL: low-density lipoprotein; HDL: high-density lipoprotein.

a density of  $2 \times 10^3$  cells/well. After adherence to the plate, the initial defining media were aspirated away and replaced with complete medium supplemented with 5'-Aza-dC (Sigma-Aldrich) in the treated group. At 24, 48, and 72 h, cell proliferation was assayed by 3-(4, 5-Dimethylthiazol-2-yl)-2, 5-diphenyltetrazolium bromide as per the manufacturer's instructions.

**Reactive oxygen species (ROS).** The intracellular ROS level was measured by ROS-specific fluorescent probe, 2',7'-Dichlorofluorescein diacetate (DCFH-DA; Beyotime Institute of Biotechnology). The collected cells, at a density of  $2 \times 10^5$  cells/ml, were resuspended in DCFH-DA and incubated in the dark at 37°C for 20 min. They were then washed with serum-free medium 3 times to remove the excessive probes. The mean fluorescence intensity (MFI) of DCF in different samples was analyzed using flow cytometry with an excitation wavelength of 488 nm and an emission wavelength of 525 nm.

**Mitochondrial membrane potential (MMP).** MMP was determined by 5,5',6,6'-tetrachloro-1,1',3,3'-tetraethylbenzimidazolycarbocyanine iodide (JC-1; Beyotime Institute of Biotechnology) staining, according to the manufacturer's instructions. Images were collected and analyzed with a laser scanning confocal microscope (Zeiss LSM 510). The value of MMP staining from each sample was expressed as ratio of red fluorescence intensity over green fluorescence intensity.

**Detection of P-gp by flow cytometry.** Analysis of cell preparations by flow cytometry (Cytomics FC-500; Beckman Coulter) was carried out using the P-gp monoclonal antibody conjugated with phycoerythrin (Biolegend). The cells ( $5 \times 10^5$ ) were incubated with the monoclonal antibody under an ice-cold chamber for 30 min with 1:20 dilution. More than 10,000 events were acquired and analyzed using computer software (CXP; Beckman Coulter).

**Western blot analyses.** Cells were washed twice with ice-cold phosphate buffered saline, scraped into 0.2 ml of buffer (50 mM Tris with pH 7.4, 150 mM NaCl, 1% Triton X-100, 1% sodium deoxycholate, 0.1% sodium dodecyl sulfate, and 0.05 mM EDTA), and incubated on ice for 20 min, followed by centrifugation at 12,000 rpm for 10 min. Protein concentrations were quantified by a BCA Protein Assay kit (Beyotime Institute of Biotechnology). Afterward, proteins were diluted to equal concentrations, boiled for 5 min, and separated by electrophoresis on 10% sodium dodecyl sulfate-polyacrylamide gel electrophoresis, and then blotted onto PVDF membranes (Milipore), which were probed with P-gp antibody overnight at 4°C. Membranes were incubated with horseradish peroxidase-conjugated secondary antibodies for 1 h at room temperature (Boster Biosciences). GAPDH was used to normalize for protein loading.

**Real-time PCR.** Total RNA was extracted through standard protocols using standard commercial kits (TRIZOL Reagent, Invitrogen). Real-time PCR were performed using SYBR Green Master mix according to the protocols of the supplier (Invitrogen). The primer sequences are shown in Table 2. The SYBR Green signal was detected by a real-time PCR machine (StepOne Real-Time PCR; ABI). The relative levels of transcript expression were quantified using the  $\Delta\Delta C_t$  method. All real-time PCR were run in triplicate and gene expression was analyzed (ABI PRISM 7900HT Sequence Detection System; Applied Biosystems).

**Bisulfite sequencing.** Bisulfite conversion was performed, as previously described<sup>27</sup>. Briefly, total genomic DNA was isolated from MSC using a kit (DNeasy Tissue Kit; Cwbiotech). Two micrograms of genomic DNA were denatured in 50  $\mu$ l by freshly prepared 0.3 M NaOH for 30 min at 42°C. After denaturation, 30  $\mu$ l freshly prepared hydroquinone (10 mM) and 510  $\mu$ l sodium bisulfite (3.6 M, pH 5.0) were added and incubated at 50°C for 16 h. Modified DNA was purified using a spin column (DNeasy Spin Column; Qiagen) and eluted in 50  $\mu$ l. This was followed by desulfonification by adding 5.5  $\mu$ l 3 M NaOH for 15 min at 37°C. Samples were neutralized by adding 33  $\mu$ l ammonium acetate (10 M, pH 7.0), followed by ethanol precipitation and resuspension in water.

PCR was performed at 95°C for 5 min followed by 40 cycles of 95°C for 30 s, 55°C for 30 s, and 72°C for 1 min, with a final extension at 72°C for 7 min. The primers used for PCR analysis are shown in Table 1. The PCR products were tested in 2% agarose gel and then cloned into the pEASY-T1 vector (TransGen Biotech). The colony PCR was undertaken to screen the positive colonies. The clones with the right sizes of PCR products were sequenced on an ABI sequencer with dye terminators (Applied Biosystems). With sequencing results of 10 clones, the methylation frequency was determined for each CpG site.

**Statistical analysis.** The statistical analysis was carried out using computer software (SPSS, version 12.0; SPSS). Significance of difference was determined using a 1-way ANOVA. Data are mean  $\pm$  SD. Probabilities < 5% ( $p < 0.05$ ) were considered statistically significant. All experiments were repeated 3 or more times.

## RESULTS

**Measurement of hMSC viability.** Figure 1A shows that cellular viability reached its peak at the dosage of 15  $\mu$ M at 72 h, and an obvious decrease in cell viability was seen when they were treated with 5'-Aza-dC at concentrations above 30  $\mu$ M. Hence, the concentration of 15  $\mu$ M was considered moderate and chosen for use in subsequent experiments.

In Figure 1B, the cellular viability in the control group was better than the GC-induced ONFH group at 3 different time points ( $p < 0.05$ ). When treated with 15  $\mu$ M 5'-Aza-dC, the cellular viability in the GC-induced ONFH group

increased by more than one-fourth, but was still lower than in the control group at 72 h ( $p < 0.05$ ).

**Decrease in ROS when treated with 5'-Aza-dC.** In Figures 2A, 2C, and 2D, the levels of ROS were higher in the GC-induced ONFH group than in the control group ( $p < 0.001$ ). After 72 h of treatment with 15  $\mu$ M 5'-Aza-dC, the ROS levels were decreased in the 5'-Aza-dC treated group (Figures 2A, 2B, 2D).

**Increase in MMP when treated with 5'-Aza-dC.** Figure 3 shows that the MMP was lower in the GC-induced ONFH group than in the control group and treatment with 5'-Aza-dC can restore the polarization state of the mitochondria, as indicated by an obvious increase in red (JC-1 aggregates)/green (JC-1 monomers) ratio.

**P-gp expression was enhanced when treated with 5'-Aza-dC.** P-gp expression was quantified by the analysis of MFI in different samples using flow cytometry with an excitation wavelength of 488 nm and an emission wavelength of 575 nm. The MFI of the GC-induced ONFH group was less than that of the control group ( $10.42 \pm 1.52$  vs  $17.46 \pm 1.91$ ;  $p < 0.01$ ). Treatment with 5'-Aza-dC can increase the expression of surface P-gp ( $14.69 \pm 2.52$ ;  $p < 0.05$ ), which was still less than that of the control group ( $p < 0.05$ ; Figures 4A, 4b, 4c, 4D, 4E). Western blot analysis revealed that the MSC in the GC-induced ONFH group showed a low level of P-gp compared to the control group. When treated with 5'-Aza-dC for 72 h, P-gp in the total protein were increased (Figure 5).

The results of the real-time PCR showed that the amount of ABCB1 transcripts in the GC-induced ONFH group was the lowest among all of the groups ( $p < 0.01$ ; Figure 4F). It reached 24-fold level at 72 h after treatment with 5'-Aza-dC, almost the same level as the control group ( $p > 0.05$ ).

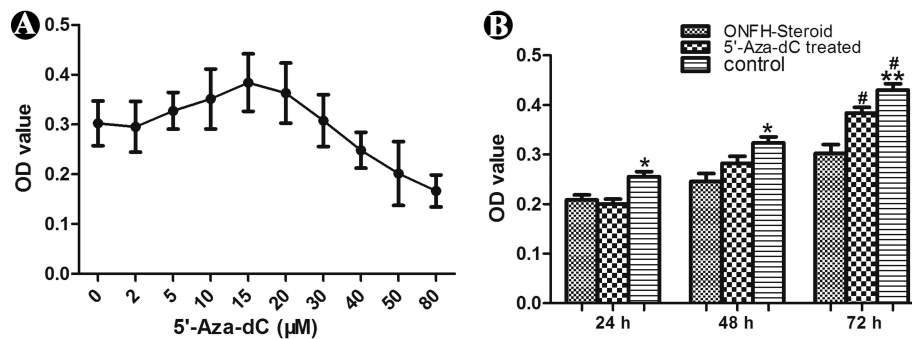
**Bisulfite sequencing.** A schematic overview of the promoter structure is shown in Figure 6. Two regions in the promoter were selected: region 1, -760 to -407, and region 2, -328 to -55. CpG hypermethylation was observed within the CpG island in the GC-induced ONFH group. After treatment with 15  $\mu$ M 5'-Aza-dC for 72 h, the methylation ratio of region 1 decreased from 18.8% to 1.8%, while the methylation level of region 2 reduced from 22.6% to 4.8%. The methylation ratio of the control group was 0.6% (region 1) and 1.7% (region 2), respectively.

## DISCUSSION

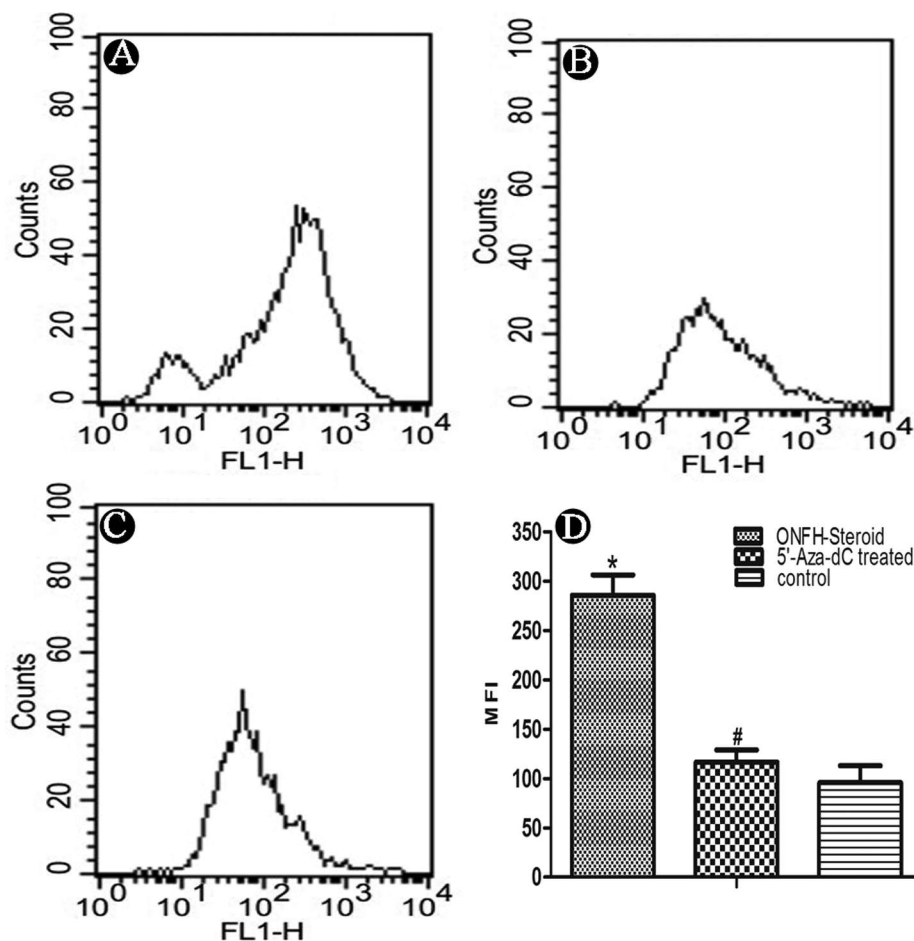
Increasing evidence reveals the presence of individual differences in steroid sensitivity, causing some patients to develop ONFH while others do not under almost the same protocol for steroid administration<sup>28</sup>. Until now, the pathophysiology of the steroid-associated ONFH had not yet been demonstrated; however, it has been determined that its pathophysiology is multifactorial<sup>1</sup>. This means that, besides environmental factors, genetic predisposition may also affect its pathogenesis. Therefore, we hypothesize that

Table 2. Primers used for real-time PCR and bisulfite sequencing.

Genes	Sequence (5'→3')	Product Size
Real-time PCR		
ABCB1-F	TTGCTGCTTACATTCAGGTTTCA	105 bp
ABCB1-R	AGCCTATCTCCTGTCGCATTA	
GAPDH-F	GGCACAGTCAAGGCTGAGAATG	143 bp
GAPDH-R	ATGGTGGTGAAGACGCCAGTA	
Bisulfite sequencing		
ABCB1-region1-F	AACCTACTCTCTAAACCCRC	273 nt
ABCB1-region1-R	GTTGGAGGTGAGATTAATTTTAGTT	
ABCB1-region2-F	TTATTTGTGGTGAGGTTGATT	353 nt
ABCB1-region2-R	ACCAAAAACTTCACACTATCC	



**Figure 1.** Dose response curves for 5'-Aza-dC treated cultures and cell proliferation assay. A. Cellular viability reached the peak at the dosage of 15  $\mu$ M at 72 h. B. The proliferation capacity of mesenchymal stem cells (MSC) at 24 h, 48 h, and 72 h. \* $p < 0.05$  vs osteonecrosis of the femoral head (ONFH) group, 5'-Aza-dC group at 24 h, 48 h; \*\* $p < 0.05$  vs 5'-Aza-dC group at 72 h; # $p < 0.01$  vs ONFH group at 72 h. Each group repeated the experiment 3 times.



**Figure 2.** Decrease in reactive oxygen species (ROS) level when treated with 5'-Aza-dC. A. The ROS levels in the osteonecrosis of the femoral head (ONFH) group. B. The ROS levels in the 5'-Aza-dC group. C. The ROS levels in the control group. D. The mean fluorescence intensity (MFI) of dichlorofluorescein was measured by flow cytometry. Data are mean  $\pm$  SD. \* $p < 0.001$  vs 5'-Aza-dC group, control group. # $p > 0.05$  vs control group. Each group repeated the experiment 3 times.

individual differences may contribute to aberrant CpG islands' hypermethylation of the ABCB1 gene and that it may be beneficial for the retardation of progressive ONFH

to restore ABCB1 expression by reversing the aberrant epigenetic modification.

In our study, we assessed methylation at CpG islands of



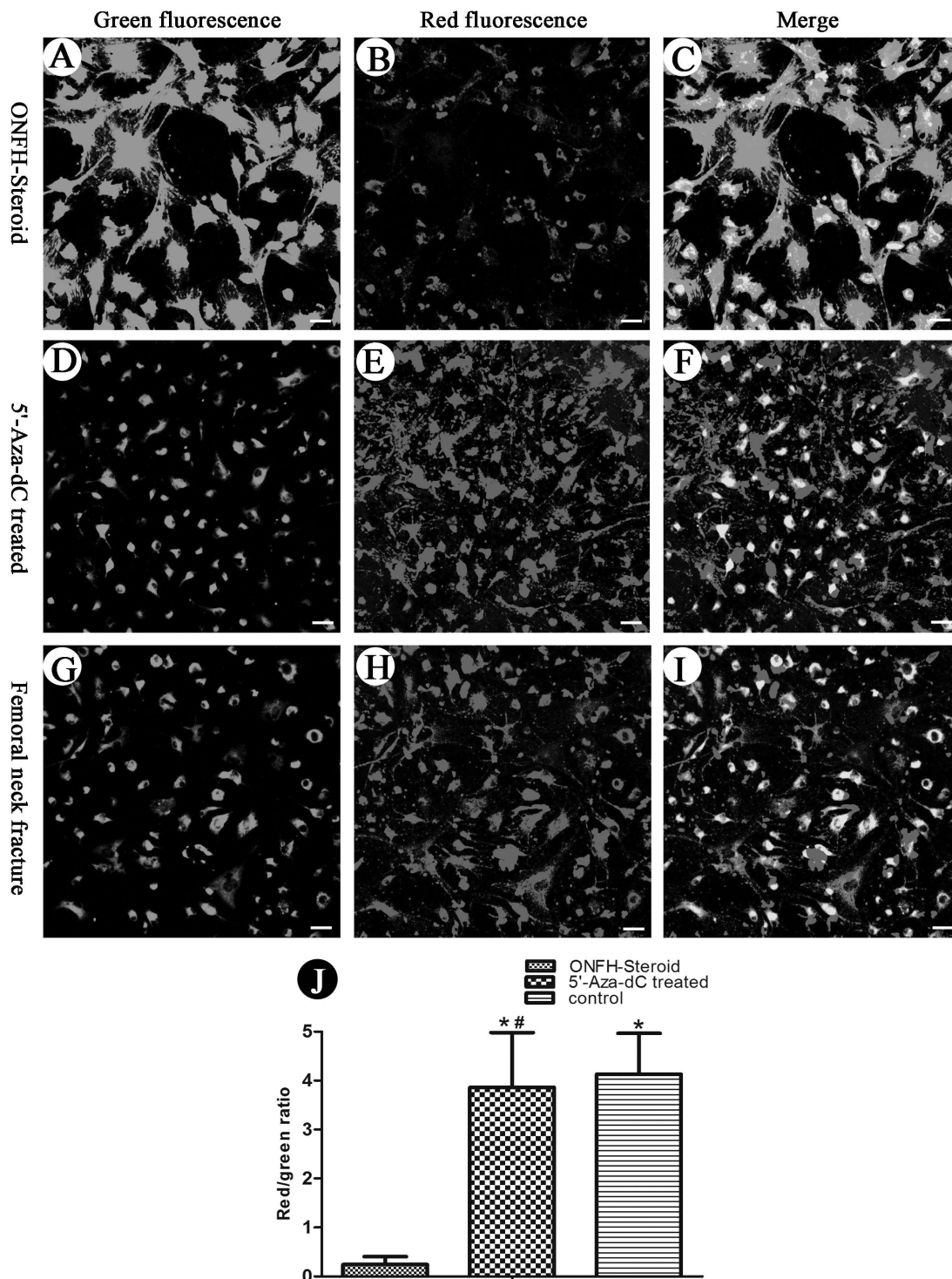


Figure 3. An increase in mitochondrial membrane potential (MMP) level by the treatment of 5'-Aza-dC. (A–C) JC-1 staining in osteonecrosis of the femoral head (ONFH) group. (D–F) JC-1 staining in the 5'-Aza-dC group. (G–I) JC-1 staining in the control group. (J) The ratio of fluorescence intensity was analyzed with a Zeiss LSM 510 laser scanning confocal microscope. Data are mean  $\pm$  SD. \* $p$  < 0.01 vs ONFH group; # $p$  > 0.05 vs control group. Each group repeated the experiment 3 times. Bar = 50  $\mu$ m.

ABCB1 gene in MSC from 47 patients with GC-induced ONFH and femoral neck fractures. We found that the methylation ratio of the ABCB1 promoter in the GC-induced

ONFH group was higher than that in the femoral neck fractures group. The amount of ABCB1 transcript and P-gp in the GC-induced ONFH group was 1/24 and one-third,

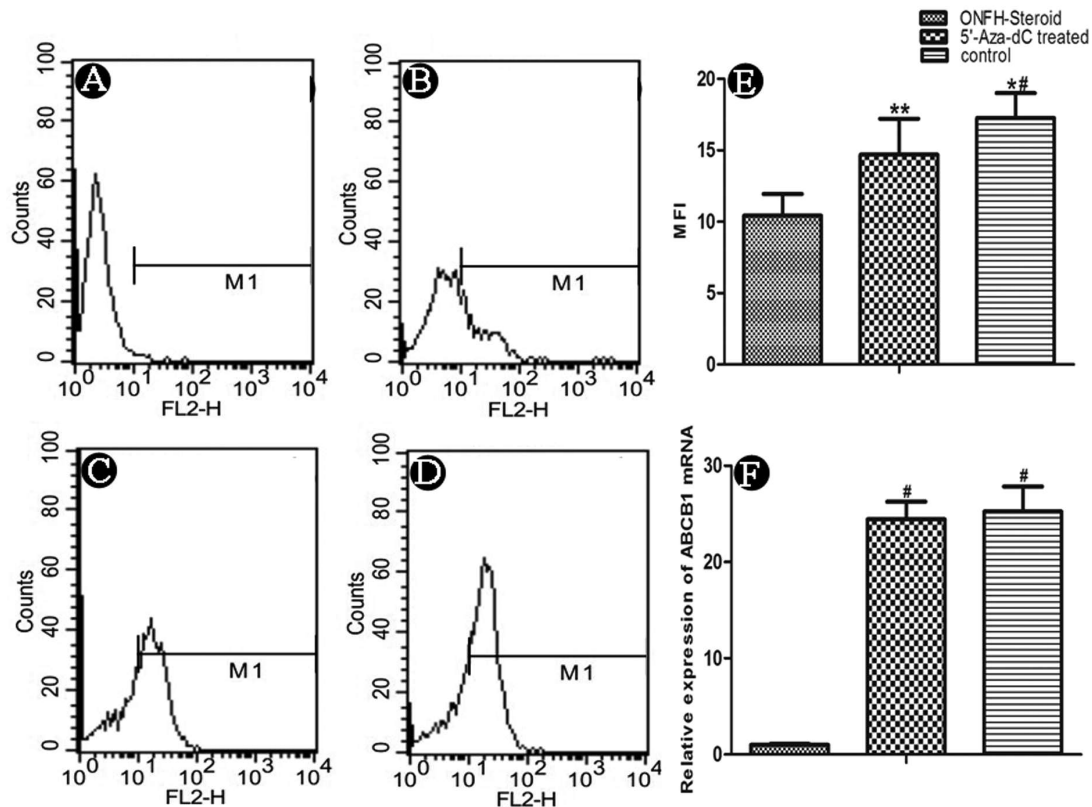


Figure 4. P-glycoprotein (P-gp) expression was enhanced by treatment with 5'-Aza-dC. A. P-gp level of negative control. B. P-gp level of osteonecrosis of the femoral head (ONFH) group. C. P-gp level of 5'-Aza-dC group. D. P-gp level of control group. E. The mean fluorescence intensity (MFI) of P-gp was measured using flow cytometry. F. ABCB1 transcript levels. Data are mean  $\pm$  SD. \* $p < 0.05$  vs 5'-Aza-dC group; \*\* $p < 0.05$  vs ONFH group; # $p < 0.01$  vs ONFH group. Each group repeated the experiment 3 times.

respectively, of that in the femoral neck fractures group. Apparently, the ABCB1 gene was partly silenced because of the hypermethylation of the promoter region in the GC-induced ONFH group. To the best of our knowledge, this is the first study to investigate the methylation status of ABCB1 promoter in patients with GC-induced ONFH.

Patients with hypermethylation of ABCB1 promoter were prone to ONFH when GC were administered. First, because GC is one of the substrates of P-gp, decreased expression of P-gp made it impossible to pump GC out in time and to protect cells from it. Therefore, GC were consistently deposited, and they exerted direct or indirect effects on the cells. Second, it was reported that over-expression of P-gp can delay the onset of apoptosis by affecting intracellular acidification that occurs early on in the apoptosis cascade<sup>29</sup>. Cells that are normally sensitive to apoptosis by Fas ligation, UV irradiation, serum starvation, or drugs can be made resistant to these caspase-dependent death stimuli by elevating intracellular pH. Thus, it is possible that increased expression of P-gp will alter intracellular pH, making the cell caspase-inactive and resistant to multiple forms of caspase-dependent death stimuli<sup>30</sup>. Conversely, downregulation of ABCB1 will easily trigger early apoptotic events.

The MSC of patients with aberrant CpG islands' hypermethylation of ABCB1 lost, at least in part, the protection of P-gp and tended to have oxidative stress injury and subsequent dysfunction when administered GC. As a result, these patients are prone to ONFH because MSC dysfunction is considered a principal mechanism in its development. As the source of osteoblasts, the decreased number and hypoproliferation of MSC is insufficient to provide enough osteoblasts to meet the needs of bone remodeling, resulting in bone necrosis.

We observed that cellular viability in the control group was remarkably higher than in the GC-induced ONFH group at all 3 different timepoints ( $p < 0.05$ ). When treated with 15  $\mu$ M 5'-Aza-dC, the cellular viability in the GC-induced ONFH group increased by more than one-fourth, while the methylation ratio was decreased to 1.8% (region 1) and 4.8% (region 2). From our ongoing research, we found that between the methylated and hypermethylated CpG patients, those with higher methylation level usually had lower MSC viability compared to age- and sex-matched controls (data not shown). From this finding, we propose that, for patients with GC-induced ONFH, there may be a connection between the methylation levels of CpG islands and MSC viability. However, a strictly designed and

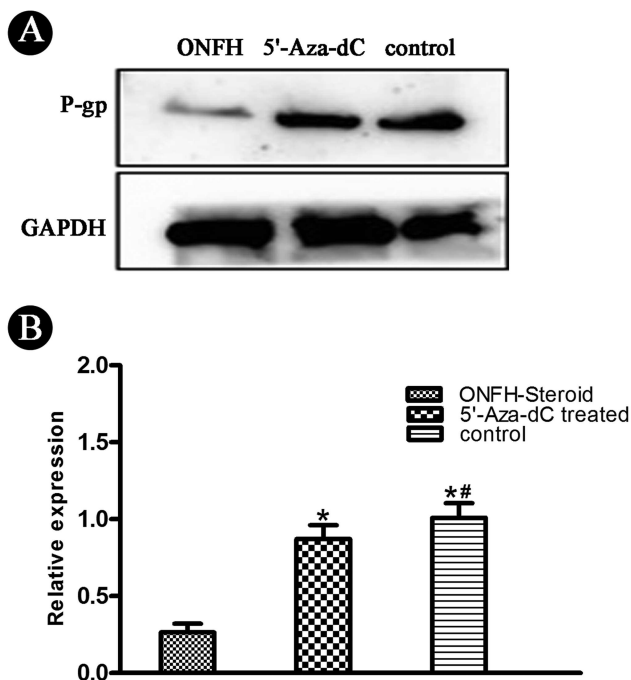


**Figure 5.** Western blot analysis. A. P-glycoprotein (P-gp) was lowly expressed in the mesenchymal stem cells of the glucocorticoid-induced osteonecrosis of the femoral head (ONFH) group, compared to the control group. When treated with 5'-Aza-dC for 72 h, P-gp in the total protein was consequently increased. GAPDH was used to normalize for protein loading. B. The histogram provided additional confirmation. Data are mean  $\pm$  SD. \* $p < 0.01$  vs ONFH group, control group. # $p > 0.05$  vs 5'-Aza-dC group. Each group repeated the experiment 3 times.

large sample study is needed.

The role of oxidative stress in GC-induced ONFH has drawn increased attention. Accumulating evidence indicates that oxidative stress is involved in the pathogenesis of ONFH<sup>31,32,33</sup>. Lu and Li showed that oxidative injury was present in the bone shortly after corticosteroid was administered and before ONFH developed<sup>31</sup>. For MSC, oxidative stress was a crucial mediator for the induction of adipogenesis when GC were administered<sup>33</sup>. It may lead to the onset of ONFH by a decrease in stem cell numbers to differentiate into osteocytes and an increase in fatty marrow and intraosseous pressure, a process that decreased arterial perfusion. P-gp has been demonstrated to modulate the accumulation of intracellular GC, and high concentrations of GC can cause oxidative stress and promote MSC adipogenesis<sup>34,35</sup>. Low expression of P-gp would increase the accumulation and effect of GC *in vivo*<sup>36</sup>. In our study, we observed that treatment with 5'-Aza-dC partially restored ABCB1 expression and concomitantly both the intracellular ROS level and MMP, 2 important indices of oxidative stress, reached almost the same levels as the control group. Correspondingly, the proliferation of MSC in the GC-induced ONFH group was also improved. We speculated that the effect of 5'-Aza-dC might be also due to attenuated intracellular availability of GC by upregulation of P-gp and the oxidative stress that happened in the MSC of GC-induced ONFH may be relieved by *de novo* P-gp expression. However, the underlying mechanism remains to be studied.

Our study has demonstrated for the first time, to our

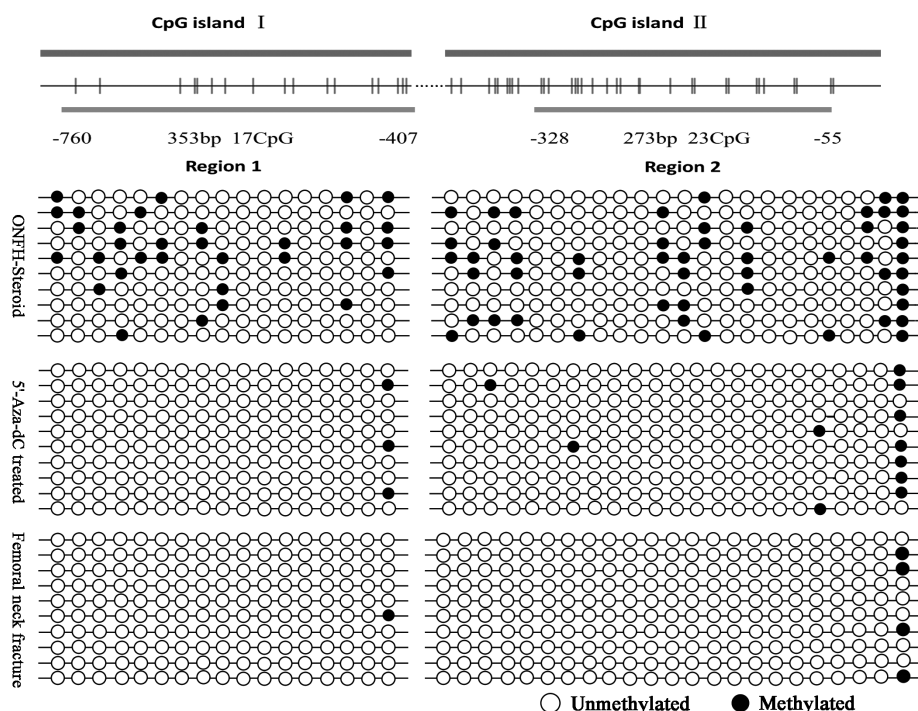


**Figure 6.** Bisulfite sequencing. Region 1 (-760 to -407 bp): the methylation ratio of the osteonecrosis of the femoral head (ONFH) group was 18.8%, 1.8% in the 5'-Aza-dC group, and 0.6% in the control group. Region 2 (-328 to -55bp): the methylation ratio was 22.6% in the ONFH group, 4.8% in the 5'-Aza-dC group, and 1.7% in the control group. Each group repeated the experiment 3 times.



knowledge, that individual differences in steroid sensitivity may be at least partially attributed to aberrant CpG islands' hypermethylation of the ABCB1 gene, and that it may be possible to decrease the risk of ONFH in patients having GC therapy or to improve the treatment by *de novo* P-gp expression. However, more specific *in vivo* studies are needed to further elucidate other mechanisms involved in the development of ONFH and their interaction.

## REFERENCES

- Mont MA, Hungerford DS. Non-traumatic avascular necrosis of the femoral head. *J Bone Joint Surg Am* 1995;77:459-74.
- Wu X, Yang S, Duan D, Liu X, Zhang Y, Wang J, et al. A combination of granulocyte colony-stimulating factor and stem cell factor ameliorates steroid-associated osteonecrosis in rabbits. *J Rheumatol* 2008;35:2241-8.
- Ko JY, Wang FS, Wang CJ, Wong T, Chou WY, Tseng SL. Increased Dickkopf-1 expression accelerates bone cell apoptosis in femoral head osteonecrosis. *Bone* 2010;46:584-91.
- Pietrogrande V, Mastommarino R. Osteopatia da prolungato trattamento cortisonico (English abstract). *Orthop Traumatol* 1957;25:791-810.
- Murata M, Kumagai K, Miyata N, Osaki M, Shindo H. Osteonecrosis in stroke-prone spontaneously hypertensive rats: effect of glucocorticoid. *J Orthop Sci* 2007;12:289-95.
- Yeh CH, Chang JK, Wang YH, Ho ML, Wang GJ. Ethanol may suppress Wnt/beta-catenin signaling on human bone marrow stroma cells: a preliminary study. *Clin Orthop Relat Res* 2008;466:1047-53.
- Drescher W, Lohse J, Varoga D, Buschmann C, Liebs T, Herdegen T, et al. Enhanced constriction of supplying arteries — a mechanism of femoral head necrosis in Wistar rats? *Ann Anat* 2010;192:58-61.
- Drescher W, Varoga D, Liebs TR, Lohse J, Herdegen T, Hassenpflug J, et al. Femoral artery constriction by norepinephrine is enhanced by methylprednisolone in a rat model. *J Bone Joint Surg Am* 2006;88:162-6.
- Urbaniak JR, Seaber AV, Chen LE. Assessment of ischemia and reperfusion injury. *Clin Orthop Relat Res* 1997;334:30-6.
- Cuadrado MJ, Lopez-Pedraza C. Antiphospholipid syndrome. *Clin Exp Med* 2003;3:129-39.
- Yun SI, Yoon HY, Jeong SY, Chung YS. Glucocorticoid induces apoptosis of osteoblast cells through the activation of glycogen synthase kinase 3beta. *J Bone Miner Metab* 2009;27:140-8.
- Chen C, Yang S, Feng Y, Wu X, Chen D, Yu Q, et al. Impairment of two types of circulating endothelial progenitor cells in patients with glucocorticoid-induced avascular osteonecrosis of the femoral head. *Joint Bone Spine* 2012;80:70-6.
- Varoga D, Drescher W, Pufe M, Groth G, Pufe T. Differential expression of vascular endothelial growth factor in glucocorticoid-related osteonecrosis of the femoral head. *Clin Orthop Relat Res* 2009;467:3273-82.
- Petronis A. Epigenetics as a unifying principle in the aetiology of complex traits and diseases. *Nature* 2010;465:721-7.
- Zhang TY, Meaney MJ. Epigenetics and the environmental regulation of the genome and its function. *Annu Rev Psychol* 2010;61:439-66.
- Iqbal M, Ho HL, Petropoulos S, Moisiadis VG, Gibb W, Matthews SG. Pro-inflammatory cytokine regulation of P-glycoprotein in the developing blood-brain barrier. *PLoS ONE* 2012;7:e43022.
- Han N, Yan Z, Guo CA, Shen F, Liu J, Shi Y, et al. Effects of P-glycoprotein on steroid-induced osteonecrosis of the femoral head. *Calcif Tissue Int* 2010;87:246-53.
- Kuribayashi M, Fujioka M, Takahashi KA, Arai Y, Hirata T, Nakajima S, et al. Combination analysis of three polymorphisms for predicting the risk for steroid-induced osteonecrosis of the femoral head. *J Orthop Sci* 2008;13:297-303.
- Matsumoto T, Kano K, Kondo D, Fukuda N, Iribe Y, Tanaka N, et al. Mature adipocyte-derived dedifferentiated fat cells exhibit multilineage potential. *J Cell Physiol* 2008;215:210-22.
- Chen J, Shi ZD, Ji X, Morales J, Zhang J, Kaur N, et al. Enhanced osteogenesis of human mesenchymal stem cells by periodic heat shock in self-assembling peptide hydrogel. *Tissue Eng Part A* 2012;19:716-28.
- Huang Y, Zheng L, Gong X, Jia X, Song W, Liu M, et al. Effect of cyclic strain on cardiomyogenic differentiation of rat bone marrow derived mesenchymal stem cells. *PLoS ONE* 2012;7:e34960.
- Sun ZB, Zhang YK, Yang SH, Jia J, Ye S, Chen D, et al. Growth differentiation factor 5 modulation of chondrogenesis of self-assembled constructs involves gap junction-mediated intercellular communication. *Dev Growth Differ* 2012;54:809-17.
- Zhang B, Yang SH, Sun ZB, Zhang Y, Xia T, Xu W, et al. Human mesenchymal stem cells induced by growth differentiation factor 5: an improved self-assembly tissue engineering method for cartilage repair. *Tissue Eng Part C Methods* 2011;17:1189-99.
- Lange C, Brunswig-Spickenheier B, Eissing L, Scheja L. Platelet lysate suppresses the expression of lipocalin-type prostaglandin D2 synthase that positively controls adipogenic differentiation of human mesenchymal stromal cells. *Exp Cell Res* 2012;318:2284-96.
- Koo KH, Kim R, Kim YS, Ahn IO, Cho SH, Song HR, et al. Risk period for developing osteonecrosis of the femoral head in patients on steroid treatment. *Clin Rheumatol* 2002;21:299-303.
- Yu M, Xiao Z, Shen L, Li L. Mid-trimester fetal blood-derived adherent cells share characteristics similar to mesenchymal stem cells but full-term umbilical cord blood does not. *Br J Haematol* 2004;124:666-75.
- Irizarry RA, Ladd-Acosta C, Wen B, Wu Z, Montano C, Onyango P, et al. The human colon cancer methylome shows similar hypo- and hypermethylation at conserved tissue-specific CpG island shores. *Nat Genet* 2009;41:178-86.
- Asano T, Takahashi KA, Fujioka M, Inoue S, Okamoto M, Sugioka N, et al. ABCB1 C3435T and G2677T/A polymorphism decreased the risk for steroid-induced osteonecrosis of the femoral head after kidney transplantation. *Pharmacogenetics* 2003;13:675-82.
- Robinson LJ, Roberts WK, Ling TT, Lamming D, Sternberg SS, Roepe PD. Human MDR 1 protein overexpression delays the apoptotic cascade in Chinese hamster ovary fibroblasts. *Biochemistry* 1997;36:11169-78.
- Johnstone RW, Cretney E, Smyth MJ. P-glycoprotein protects leukemia cells against caspase-dependent, but not caspase-independent, cell death. *Blood* 1999;93:1075-85.
- Lu BB, Li KH. Lipoic acid prevents steroid-induced osteonecrosis in rabbits. *Rheumatol Int* 2012;32:1679-83.
- Ichiseki T, Matsumoto T, Nishino M, Kaneuji A, Katsuda S. Oxidative stress and vascular permeability in steroid-induced osteonecrosis model. *J Orthop Sci* 2004;9:509-15.
- Liu H, Yang X, Zhang Y, Dighe A, Li X, Cui Q. Fullerol antagonizes dexamethasone-induced oxidative stress and adipogenesis while enhancing osteogenesis in a cloned bone marrow mesenchymal stem cell. *J Orthop Res* 2012;30:1051-7.
- Miyanishi K, Yamamoto T, Irita T, Yamashita A, Motomura G, Jingushi S, et al. Effects of cyclosporin A on the development of osteonecrosis in rabbits. *Acta Orthop* 2006;77:813-9.
- Kralli A, Yamamoto KR. An FK506-sensitive transporter selectively decreases intracellular levels and potency of steroid hormones. *J Biol Chem* 1996;271:17152-6.
- Miyanishi K, Yamamoto T, Irita T, Yamashita A, Motomura G, Jingushi S, et al. Effects of tacrolimus (FK506) on the development of osteonecrosis in a rabbit model. *Immunopharmacol Immunotoxicol* 2008;30:79-90.